JTTEE5 7:513-520

PEER REVIEWED

Experimental Studies of Twin-Wire Electric Arc Sprayed Zinc/Aluminum Alloy Coatings

D.J. Varacalle, Jr., D.P. Zeek, V. Zanchuck, E. Sampson, K.W. Couch, D. Benson, and G.S. Cox

(Submitted 29 October 1997; in revised form 12 May 1998)

An experimental study of twin-wire electric arc spraying of zinc/aluminum alloy coatings demonstrates the suitability of the systems for anticorrosion applications. Experiments were conducted using Box-type, fractional-factorial designs. The process parameters that were varied include nozzle diameter, current, spray distance, and system pressure. The experiments were designed to display the range of processing conditions and their effect on the coating. The coatings were characterized with bond strength and deposition efficiency tests and optical metallography. Coating characteristics were quantified with respect to roughness, porosity, thickness, bond strength, and microstructure. Performance evaluation of the coatings was quantified with accelerated corrosion testing. A parameter-property-performance relationship has been developed for each material system. This paper presents the results of material systems 85Zn/15Al and 70Zn/30Al.

Keywords Box, characterization, coatings, corrosion resistance, regression analysis, twin-wire, 85/15

1. Introduction

The twin-wire electric arc (TWEA) process can be traced back to 1914 (Ref 1), when Schoop and his colleague Bauerlin performed their initial experiments with electric heating wires. The key advantages of the process are higher output and lower cost than other processes. Two wires are brought close together and an electric arc is struck between them. Typical direct current (dc) voltages are between 20 and 35 V, with current ranging up to 350 A and, in some cases, more. Wire feed rate is governed by the system current. The arc developed between the two wires causes the wire tips to melt and superheat. An atomizing gas, typically air, is delivered to these two wires to strip off small droplets of molten metal, transferring kinetic energy to the droplets. Typical air flow rates range from 850 to 1699 L/min (30 to 60 standard cubic feet per minute, or scfm). It is common to spray with either nitrogen or argon to reduce the formation of oxides on the molten droplets. In general, any material that is electrically conductive and can be made into a wire can be sprayed with a TWEA device. The Tafa Model 9000 TWEA arc spray gun was used in the study.

Zinc and aluminum alloy coatings find widespread applications in the automotive, transportation, and aircraft industries for anticorrosion applications. The two material systems are commonly used for anticorrosion applications in infrastructure industries. The purpose of this study was to develop a methodology to generate baseline data to optimize the previously mentioned material systems for the protection of steel. The study also furthers the understanding of the mechanisms involved in the formation of TWEA coatings by determining how process parameter variations affect the process dynamics, the subsequent coating properties, and the coating performance.

Empirical studies were conducted to determine whether zinc/aluminum alloy coatings sprayed with a TWEA spray system could perform as corrosion resistant coatings for infrastructure, especially site-specific applications at the Idaho National Engineering and Environmental Laboratory (INEEL). Much of the waste stored at the INEEL is stored in Department of Transportation type A-certified, 55 gal steel drums. Degradation by corrosion of many containers stored at the site has raised concern regarding the safe storage, handling, transportation, and disposal of this waste. Technology and equipment for refurbishing waste containers at the INEEL has been selected. The method involves surface preparation techniques, metal sprayed coatings, and sealing the coatings with polymers. In this study, the coating designs were based on determining the highest corrosion resistance that could be obtained with the process.

The selection of a thermal spray coating depends on the desired service life, environmental envelope, operating duty, and the maintenance and repair support provided during the life cycle. Zinc and aluminum are widely used as spray coatings for steel because they offer corrosion protection by several mechanisms. Foremost is the physical barrier of having the coating on the substrate. Then, zinc and aluminum are more negative in electrochemical potential than steel (Ref 2). Thus, if a crack occurs in the coating, a galvanic couple is created between the zinc or aluminum coating and the steel. The coating will act as the anode, preferentially corroding rather than the steel and providing cathodic protection.

2. Experimental Procedure

The TWEA spray process was chosen for this application because it can produce economical, high-purity, low-porosity coatings with high bond and interparticle strength. A Tafa, Inc., Model 9000, TWEA spray system and commercially available

D.J. Varacalle, Jr. and **D.P. Zeek,** Idaho National Engineering Laboratory, Idaho Falls, Idaho 83415; **V. Zanchuck** and **E. Sampson,** Tafa, Inc., Concord, NH 03301; **K.W. Couch** and **D. Benson,** Protech Lab. Corp., Cincinnati, OH 45241; and **G.S. Cox,** ITI Anti-Corrosion, Inc., Houston, TX 77036. Contact e-mail: djr@inel.gov.

wire (prealloyed 85Zn/15Al, Tafa 02A; zinc, 02Z; aluminum, 01T) were used. A Box-type (Ref 3) fractional-factorial statistical design of experiment (SDE) was conducted for the 85/15 wire alloy system, and a pseudo-alloy (70Zn/30Al) was achieved by using one spool of 02Z zinc and one spool of 01T aluminum in the TWEA apparatus. The Box analysis was performed with a commercial software package, Design-Ease (Ref 4), on the measured responses.

Table 1 presents a fractional-factorial design. The design constitutes a one-half replicate of four factors in eight experiments. Each variable has two levels selected to band around the nominal settings (experiments 1 through 8) to demonstrate the processing capabilities at a variety of stable processing conditions. Centerpoint experiments (9 through 14) were also included to independently evaluate the process variation. In the design, all main effects are clear of two-factor interactions, but two-factor interactions are aliased with one another.

The process parameters varied in the experiments included orifice diameter (blue nozzle cap = 0.953 cm (0.375 in.), green nozzle cap = 0.767 cm (0.302 in.), gun pressure (i.e., air flow rate), current, and spray distance (SD). These process parameters were chosen because they strongly affect the droplet velocity and temperature and, thus, the resulting coating. Voltage was 21 V for the 85/15 experiments and 27 V for the 70/30 experiments. Air was used as the primary and shroud gas. Wire injection was internal to the gun and was directed parallel to the flow. Wire feed rate varied proportionally with the system current. The wire feed rates were 38.2 kg/h (17.3 lb/h) (100 A), 80.3 kg/h (36.5 lb/h) (200 A), and 122.8 kg/h (55.8 lb/h) (300 A) for the 85/15 experiments and 22.4 kg/h (10.2 lb/h) (100 A), 49.3 kg/h (22.4 lb/h) (200 A), and 79.6 kg/h (36.2 lb/h) (300 A) for the 70/30 experiments.

An x-y manipulator ensured constancy of the standoff distance and repeatability in the experiments. The traverse x-motion rate was 40.6 cm/s (16 in. per s). A y step of 0.32 m (0.125 in.) was used. Sixteen traverses per pass were taken. Table 1 shows the number of passes used to fabricate the coatings.

The wire was thermal sprayed onto low-carbon steel coupons (10.2 by 15.2 by 0.32 cm, or 4 by 6 by 0.125 in.) cooled by air jets on the back side. The deposition side of each coupon was grit blasted with No. 36 alumina grit prior to spraying the surface. A maximum roughness (i.e., average amplitude) of 0.05 mm (2 mil) was obtained for the substrates for the coupons used for the met mounts. A maximum roughness of 0.076 mm (3 mil) was obtained for the substrates for the coupons used for accelerated corrosion testing. Roughness of the substrates was measured with profile replica tape and a micrometer.

3. Coating Characterization

Coatings were characterized and evaluated by a number of techniques for the two material systems. These include bond strength tests, optical metallography, image analysis, surface profilometry, and deposition efficiency. Characterization of the coatings yielded the physical, chemical, and mechanical properties of the various coatings, including thickness, bond strength, roughness, porosity, oxide content, and deposition efficiency. Attributes were measured on metallographically prepared cross sections of each coating.

Porosity and oxide content were determined using image analysis (i.e., the differential interference-contrast technique). A Leco 3001 image analyzer (Leco Corp., Saint Joseph, MI) with a Nikon Epiphot PMG-3 metallograph (Nikon Inc., Melville, NY) was used for the metallurgical mounts. A magnification of 500× was used to maximize contrast between the pores and the surrounding coating and to obtain sufficiently imaged pore size to ensure accuracy of results. Each coating was examined for bulk porosity and oxide content at ten locations. The porosities of the 85/15 coatings range from 0.6 to 5.8%, while the porosities of the 70/30 coatings range from 1.4 to 8.7% (Table 2). The same image analysis procedure was used to measure oxide content. After the coatings were measured for porosity, the oxide content was obtained by subtracting the porosity value from the measured porosity plus oxide value at each location. These values are also included in Table 2 for the 85/15 alloy, which ranged from 0.3 to 3.9%. The oxide content of the 70/30 coatings could not be determined after polishing, due to oxidation of the zinc phase and the presence of phase boundaries.

Thickness measurements were obtained using image analysis with the metallograph. The image system is equipped with a ruler tool. The system scale is first calibrated through use of a

Table 1 TWEA coating experiments

Run	Gun P		Current,	Spray Distance		Nozzle cap(a)	Passes(b)	Passes(c)
	MPa	psi	A	cm	in.			
1	0.28	40	100	7.62	3	Blue	2	3
2	0.55	80	100	7.62	3	Green	2	3
3	0.28	40	300	7.62	3	Green	1	1
4	0.55	80	300	7.62	3	Blue	1	1
5	0.28	40	100	17.8	7	Green	2	3
6	0.55	80	100	17.8	7	Blue	2	3
7	0.28	40	300	17.8	7	Blue	1	1
8	0.55	80	300	17.8	7	Green	1	1
9	0.41	60	200	17.8	5	Blue	1	2
10	0.41	60	200	12.5	5	Green	1	2
11	0.41	60	200	17.8	5	Blue	1	2
12	0.41	60	200	17.8	5	Green	1	2
13	0.41	60	200	17.8	5	Blue	1	2
14	0.41	60	200	17.8	5	Green	1	2

(a) Diameter: blue = 0.953 cm; green = 0.767 cm. (b) Passes for 85/15 alloy. (c) Passes for 70/30 system

stage micrometer traceable to the National Bureau of Standards; the micrometer is imaged through the microscope with the appropriate objective lens. When the system has been calibrated, the ruler tool is simply stretched from the top of the coating to the bottom at several locations and an average value reported. Average thicknesses ranged from 0.2 to 0.53 mm (8 to 21 mils) for the 85/15 coatings and 0.17 to 0.51 mm (6.6 to 20 mils) for the 70/30 coatings.

Surface roughness was determined using a WYKO RST white light interferometer (WYKO Corp., Tucson, AZ). The average roughness was calculated per ANSI standard B46.1 as the average departure y_i from the mean y. Average roughness ranged from 5.9 to 9.3 mm for the 85/15 coatings and 6.5 to 13.2 mm for the 70/30 coatings.

Deposition efficiency (DE) for selected coatings (experiment 10) was determined with conventional techniques by measuring the amount of sprayed metal deposited for an allotted time for the optimum design coatings of this study. Deposition efficiency of the wire was 56.2% for the 85/15 coatings and 45.7% for the 70/30 coatings. Note that the DE experiments were conducted on 10.2 by 15.2 cm (4 by 6 in.) coupons cooled by air from the back. One experiment was conducted for each wire system. The reported wire deposition efficiencies could be 15 to 20% higher if sprayed on larger substrates (e.g., 30.5 by 30.5 cm, 12 by 12 in.).

Bond strength measurements were conducted using two methods. A wide variance in bond strength is expected because the sprayed samples illustrated in Table 1 were sprayed with significantly different processing parameters. Bond strength measurements were first conducted only for the centerpoint experiments following the test procedure described by ANSI/ASTM standard C 633-79. The coatings were sprayed onto 38 mm diameter stainless-steel rods grit blasted and cleaned prior to deposition of coating. An adhesive was then used to bond the rods. The strength of the joints were tested using a tensile testing machine. The bond strength average was 17.17 MPa (2490 psi) for the 85/15 coatings; the 70/30 coatings averaged 16.2 MPa (2350 psi). Bond strength studies were also conducted using a portable adhesion tester (PATTI, Pneumatic Adhesion Tensile Testing Instrument; KTA-Tator, Inc.) described by ASTM standard D 4541. Five tests were conducted for each experiment illustrated in Table 1 and averaged for nominal bond strength. The materials were sprayed onto light carbon steel substrates. Each coupon was grit blasted with No. 36 alumina grit prior to spraying the surface to obtain a surface roughness (i.e., amplitude) of 76.2 μm (3 mils). An adhesive was

Table 2 Characterization results for 70Zn/30Al and 85Zn/15Al systems

	70/30 system						
Experiment	Porosity, %	Thickness, mm	Thickness, mil	Roughness, μm	Bond strength, MPa	Bond strength, psi	Corrosion resistance
01	8.7	0.73	9.0	10.1	7.58	1100	88
02	3.9	0.22	8.6	8.0	6.46	937	29
03	4.5	0.31	12.0	13.2	5.61	814	25
04	2.4	0.31	12.0	8.9	6.18	896	54
05	5.5	0.25	10.0	8.4	7.86	1140	71
06	4.0	0.17	6.6	6.7	9.55	1385	98
07	6.6	0.20	8.0	7.7	10.11	1467	56
08	2.1	0.29	11.6	7.2	7.58	1100	45
09	4.2	0.32	12.6	11.1	8.71	1263	87
10	1.4	0.51	20.0	8.6	9.27	1344	7
11	4.0	0.28	11.0	9.2	10.11	1467	34
12	3.0	0.36	14.0	6.5	6.74	978	35
13	5.1	0.33	13.0	7.7	9.55	1385	70
14	3.3	0.38	15.0	7.1	7.86	1140	36
7030C (CE)	3.2	0.39	15.2	...	7.86	1140	98

	85/15 system							
Experiment	Porosity, %	Oxide content, %	Thickness, mm	Thickness, mil	Roughness, μm	Bond strength, MPa	Bond strength, psi	Corrosion resistance
01	5.0	2.2	0.38	15.0	9.3	6.74	978	87
02	0.6	0.8	0.41	16.0	6.2	...	...	98
03	4.6	3.1	0.38	15.0	7.5	7.3	1059	74
04	1.0	0.3	0.53	21.0	8.6	7.86	1140	49
05	2.3	2.7	0.36	14.0	6.3	...	...	89
06	2.9	2.3	0.36	14.0	7.6	6.74	978	30
07	5.8	3.9	0.38	15.0	9.1	...	...	43
08	1.5	0.4	0.47	18.6	6.6	5.61	814	62
09	1.1	0.9	0.46	18.0	7.5	5.61	814	11
10	1.5	0.6	0.28	11.0	5.9	5.89	855	38
11	2.8	0.9	0.20	8.0	8.0	7.58	1100	54
12	1.2	0.4	0.32	12.6	5.9	5.61	814	43
13	4.0	2.0	0.28	11.0	8.2	7.3	1059	20
14	1.2	0.6	0.33	13.0	6.4	5.61	814	53
8515C (CE)	2.3	2.1	0.47	18.7	...	10.11	1467	98

Thickness, T; roughness, R; porosity, p; oxide content, O; bond strength, BS; corrosion resistance, CR; nondimensional; confirmation experiment, CE

then used to bond a pull stub to the coatings. The bond strength ranged from 5.61 to 7.86 MPa (814 to 1140 psi) for the 85/15 coatings, and 5.61 to 10.11 MPa (814 to 1467 psi) for the 70/30 coatings, using the PATTI instrument. The bond strength of the confirmation coatings was 10.11 MPa (1467 psi) for the 85/15 coating and 7.86 MPa (1140 psi) for the 70/30 coating, using the PATTI instrument.

Image analysis revealed differences in the microstructures of the experiments. Based on the criteria of low porosity (<3%) and oxide (<3%) content, many of the 70/30 and 85/15 coatings were graded as very good in quality. There are substantial differences between the microstructures of the optimum (i.e., confirmation) 85/15 and 70/30 coatings. Figure 1 illustrates the microstructure (200×) for confirmation coating 7030C. The coating has discernible porosity homogeneously dispersed throughout the coating matrix. Some large pores are evident and no cracking occurred. Figure 2 (200×) illustrates the microstructure for confirmation coating 8515C. The coating has smaller pores than the 70/30 coating, with a more homogeneous distribution. No cracking nor unmelted particles were evident. Higher magnification views of these microstructures indicate completely different morphologies and distributions.

The design coatings were analyzed using wet chemistry procedures for zinc and aluminum content. The 70/30 coating (experiment 7030C) consisted of 69% zinc and 31% aluminum; the 85/15 coating (experiment 8515C) consisted of 81% zinc and 19% aluminum.

4. Coating Performance Evaluation

Laboratory testing of 70/30 and 85/15 test panels was performed to evaluate the ability of the materials to resist corrosion when subjected to a salt spray environment for 1000 h in accordance with ASTM B 117-95. Fourteen samples of each material were tested in accordance with the test matrix shown in Table 1.

The evaluation procedure involved periodic and final preparations: (a) Test panels were removed from the salt spray and photographed at each 100 h interval through 900 h. (b) After 1000 h, the test panels were cleaned with 10% HCl for one minute to remove salts and corrosion products from the surface. (c) The test panels were then qualitatively evaluated for surface pitting to find the percentage of surface area exhibiting pitting or other corrosive activity, to evaluate erosion of coating from the edges and to determine whether the steel substrate was exposed.

Panels were then evaluated in order of performance relative to pitting and surface area evaluation parameters, and ranked from 1 to 14 for each material system. Weighting factors were assigned arbitrarily to the evaluation parameters as follows: surface area involved, erosion from edge, and steel substrate exposed (Ref 4). Erosion from the edge and steel substrate exposed had a minimal effect on the coating performance. The final value for corrosion resistance (CR), that is, summation of evaluation parameter ranks, is illustrated in Table 2. The highest value of CR is the most corrosion-resistant coating. The CR average of 70/30 coatings was 52.5; the CR average of the 85/15 coatings was 56.4, indicating the 85/15 coatings had a slightly higher corrosion resistance.

5. Discussion of Box Fractional-Factorial Experiment Design

Once experiments were conducted to ascertain important process parameters, statistically designed experiments were conducted for the two material systems to determine the parameter space for optimization. The studies used a two-level, three-variable, one-half fractional-factorial design. The Box-type statistical design of experiment methodology is an efficient means of determining broad-based factor effects on measured attributes. This method statistically delineates the impact of each variable on the measured coating characteristics across all combinations of other factors. By examination of the optimum levels of the process parameters, a design coating was obtained for the particular application for both material systems.

After the experiments were conducted, the data were analyzed with the Design-Ease computer program for the fractional-factorial design. By using the variance of the process parameter divided by the total variance, an influence variable, %I, can be obtained to determine which parameters are the most

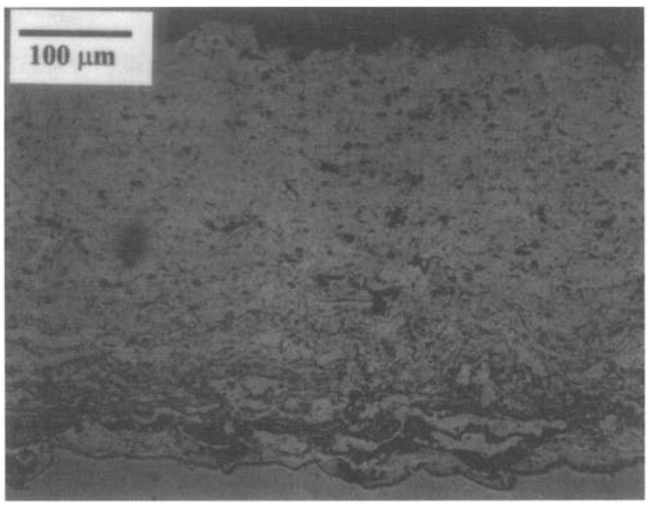

Fig. 1 Photomicrograph for confirmation coating 7030C. 200×. (Art has been reduced to 73% of its original size for printing.)

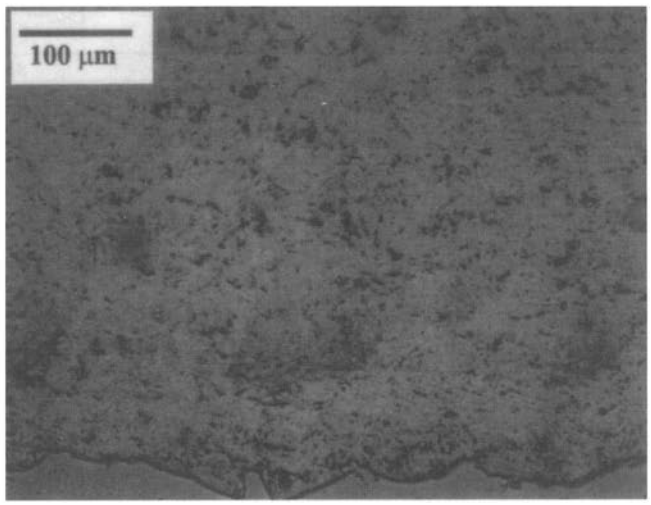

Fig. 2 Photomicrograph for confirmation coating 8515C. 200×. (Art has been reduced to 73% of its original size for printing.)

influential on the coating attributes. This, in conjunction with the optimal level for each process parameter and the magnitude of the effect, E, on the coating attribute will dictate the process parameters. Tables 3 and 4 illustrate the results of the Box effects analyses for the 70/30 and 85/15 systems. The optimum coating for this application would have, in order of priority, high corrosion resistance, high bond strength, and low roughness (i.e., smooth). Whether low porosity combined with low oxide content enhances corrosion resistance is an important question. Intuitively, low porosity and low oxide content would appear to enhance corrosion resistance. However, from Tables 3 and 4, trend analysis indicates the opposite, that high porosity combined with high oxide content enhances corrosion resistance.

The effects analysis illustrated in Tables 3 and 4 was used to determine the optimum process parameters for the 70/30 and 85/15 wire systems. The optimum coating was based on the highest corrosion resistance that could be obtained for each material. Low porosity and low oxide content were a secondary consideration. Because bond strength had a relatively small variance, it was discounted. The smoothness of the coating was inconsequential for this application, because the metal coating will either be sealed with a paint or a polymer coating.

For the 70/30 system, corrosion resistance was most influenced by nozzle diameter. Porosity was most influenced by pressure. The combination of the blue nozzle cap, 0.55 MPa (80 psi) gun pressure, a current of 100 A, and a 17.8 cm (7 in.) spray distance was predicted to produce the most corrosion-resistant 70/30 coatings with low porosity, intermediate roughness, and high bond strength. Confirmation run 7030C verified the design process parameters and produced a coating with the highest corrosion resistance of the series (i.e., CR = 98).

For the 85/15 system, corrosion resistance was affected primarily by nozzle diameter, with current and spray distance exhibiting a significant secondary effect. Porosity and oxide content were most influenced by pressure. The combination of the green nozzle cap, 0.55 MPa (80 psi) gun pressure, a current of 100 A, and a 7.62 cm (3 in.) spray distance was predicted to produce the most corrosion resistant 85/15 coatings with low porosity, low oxide content, low roughness, and intermediate bond strength. Confirmation run 8515C verified the design process parameters and produced a coating with the highest corrosion resistance of the series (i.e., CR = 98).

The mechanisms forming the two coating systems were completely different. The 85/15 system was prealloyed, resulting in a completely homogeneous matrix of zinc and aluminum. The 70/30 system, conversely, was a matrix of separate zinc and aluminum lamellae. Despite these differences, the two material systems exhibited very similar coating properties and performance.

Once the effects analysis was completed, the analysis of variance (ANOVA) calculations were then conducted for each specific coating attribute to develop a parameter-property relationship for each material for the range of parameters illustrated in Table 1. As an example, Eq 1 illustrates the linear regression equation for porosity for the 85/15 coatings using the green cap orifice: P is in psi; where A is in amperes, and SD is in inches.

$$P_{8515} = 6.66 - 0.0731*P \quad \text{(Eq 1)}$$

This model yielded an F value (i.e., the comparison of the treatment variance with the error variance) of 11.87 and a probability value of 2.3% (i.e., the probability that the model terms are not robust). Also, the coefficient of variation (CV) was small (0.395), indicating that the error was relatively small. These values indicate that the regression model was correct for the porosity attribute. The statistical analysis indicates very small residual values (i.e., actual minus predicted) for the equation (i.e., 0.07 to 1.55), which was the criteria for the model.

Equations 2 and 3 illustrate the linear regression equations for oxide content and roughness for the 85/15 system as a function of the process parameters using the green cap orifice.

$$O_{8515} = 1.7 + 0.0056*P + 0.0165*A - 0.00028*P*A \quad \text{(Eq 2)}$$

Table 3 Results of the Box SDE 70/30 analysis

Processing factor: desired attribute	Pressure, E/%I/MPa	Current, E/%I/A	Spray distance, E/%I/cm	Nozzle D, E/%I/cap
1 High corrosion resistance	-3.5/0.4/0.28	-26.5/20.4/100	18.5/10.0/17.8	-45.2/59.3/blue
2 Low porosity	-3.2/54.0/0.55	-1.6/13.7/300	-0.3/0.5/17.8	-2.1/23.7/green
2a High porosity	-3.2/54.0/0.28	-1.6/13.7/100	-0.3/0.5/7.6	-2.1/23.7/blue
3 High bond strength	-50.8/1.2/0.28	-71.2/2.3/100	336.3/52/17.8	-285.4/37.2/blue
4 Low roughness	-2.1/31.9/0.55	1.0/6.4/100	-2.5/44.364/17.8	-0.5/1.4/green

Table 4 Results of the Box SDE 85/15 analysis

Processing factor: desired attribute	Pressure, E/%I/MPa	Current, E/%I/A	Spray distance, E/%I/cm	Nozzle D, E/%I/cap
1 High corrosion resistance	-13.5/8.2/0.28	-19.0/16.2/100	-21.0/19.8/7.6	30.8/42.6/green
2 Low porosity	-2.9/57.9/0.55	0.5/1.9/100	0.3/0.7/7.6	-1.8/22.7/green
2a High porosity	-2.9/57.9/0.28	0.5/1.9/300	0.3/0.7/17.8	-1.8/22.7/blue
3 Low oxides	-2.0/62.9/0.55	-0.1/0.1/300	0.75/8.1/7.6	-0.7/8.4/green
3a High oxides	-2.0/62.9/0.28	-0.1/0.1/100	0.7/8.1/17.8	-0.7/8.4/blue
4 High bond strength	7.7/0.1/0.55	142.0/11.6/300	-130.0/9.7/7.6	-301.0/52.0/blue
5 Low roughness	-0.8/8.1/0.55	0.6/4.6/100	-0.5/3.2/17.8	-2.6/82.4/green

Magnitude of effect, E; influence variable, %I

$$R_{8515} = 7.88 - 0.02*P \quad \text{(Eq 3)}$$

Equations 4 and 5 illustrate the corresponding linear regression equations for porosity and roughness for the 70/30 system as a function of the process parameters using the green cap orifice.

$$p_{7030} = 8.53 - 0.05*P - 0.0081*A \quad \text{(Eq 4)}$$

$$R_{7030} = 15.2 - 0.054*P + 0.637*\text{SD} \quad \text{(Eq 5)}$$

At this juncture, a linear process parameter/coating attribute relationship was established. Multiple regression analysis was then required to develop the relationship between the coating attributes and the coating performance (i.e., corrosion resistance). In this manner, the complete parameter/property/performance relationship could be defined.

6. Regression Analysis

Sequential regression analysis was used to establish a relationship between the process parameters, the coating microstructural attributes, and the coating corrosion performance. Linear, quadratic, and cubic regression analyses were used for the two-wire systems, with the criteria of minimum residuals determining the choice of the equations.

The linear regression analysis from the characterization ANOVA established the relationship between the process parameters (i.e., orifice diameter, gun pressure, current, and spray distance) and the dependent variables of porosity and oxide content.

The Minitab code (Ref 5) was used to establish the relationship between the microstructural attributes of porosity and oxide content for the 85/15 system and porosity for the 70/30 system and the dependent variable of corrosion resistance. Unfortunately, the scarcity of data limited identification of a correlation. As Tables 3 and 4 indicate, there is no clear correlation for the attributes of porosity and oxide content with the qualitative corrosion resistance for the two alloy systems of this study, and the supplementary aluminum and zinc wire systems. Figures 3 and 4 illustrate the corrosion resistance as a function of porosity (Fig. 3) and oxide content (Fig. 4). It is obvious that the limited qualitative data render correlation difficult and possibly misleading.

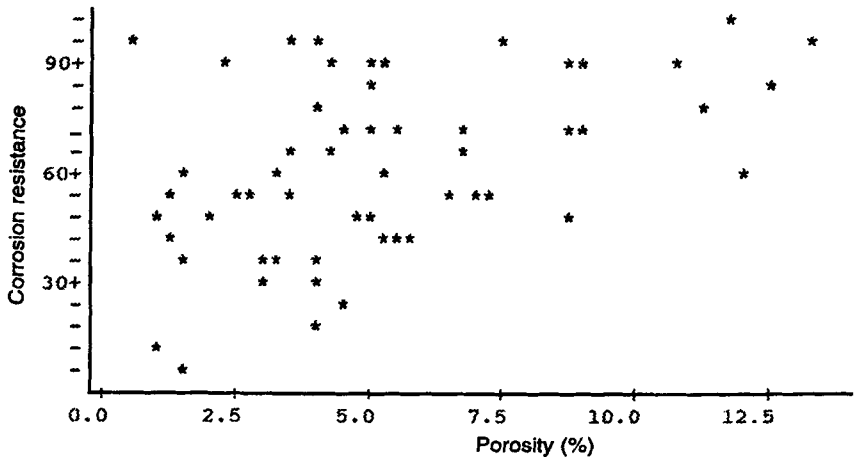

Fig. 3 Corrosion resistance as a function of porosity

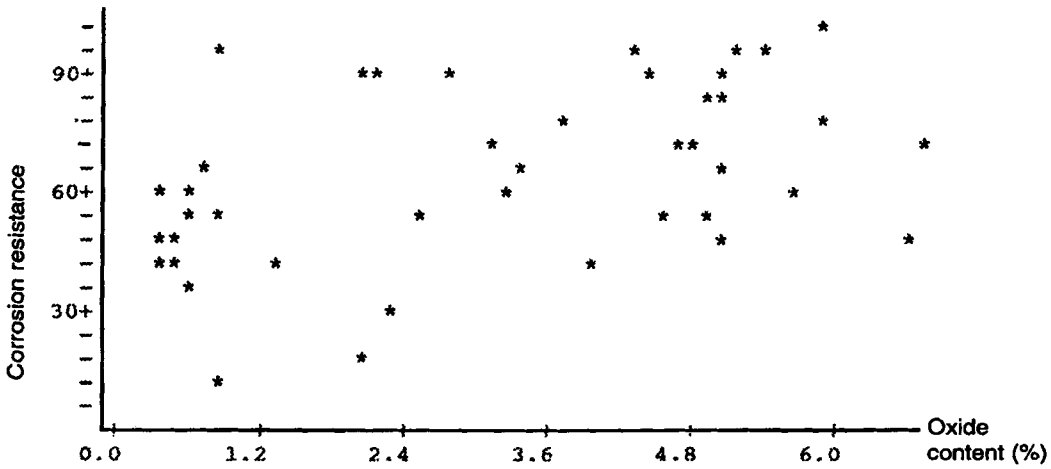

Fig. 4 Corrosion resistance as a function of oxide content

Equations 6 and 7 illustrate the equations derived from the regression analysis for the 85/15 and 70/30 wire systems, which illustrate the property/performance relationship. The equations signify the corrosion resistance for the experiments of this study as a function of the coating attributes (i.e., porosity, p, and oxide content, O, percentage) for the range of parameters illustrated in Table 1.

$$CR_{85/15} = -926 + 116*O + 214*p + 43.6*O2 + 250/O + 599/p - 48.7/O2 - 154/p2 - 68.1*O*p \quad \text{(Eq 6)}$$

$$CR_{70/30} = -173 + 35.2*p - 1.41*p2 + 552/p - 510/p2 \quad \text{(Eq 7)}$$

where O and p are in percent.

Figures 5 and 6 illustrate the predicted corrosion resistance as a function of the coating attributes of porosity and oxide content for the 85/15 system and porosity for the 70/30 system. As Fig. 5 shows, the corrosion resistance for 85/15 increases slightly as porosity and oxide content increase, and it is at a maximum at the highest porosity and oxide content. The 70/30 alloy shows similar trends, as illustrated in Fig. 4, where the corrosion resistance increases significantly with increasing porosity (i.e., a 40 point CR increase from 2% to 9.5% porosity). These trends may indicate the actual dynamics occurring in the corrosion process. Higher porosity may induce higher corrosion rates in the upper layers of the coating, which then inhibits further corrosion, whereas a lower porosity coating may allow the corrosion to penetrate further into the coating and thus enhance corrosion to the base material. However, based on the results from the effects analysis presented in Tables 3 and 4 and the subsequent confirmation testing, the authors believe the combination of lower porosity and oxide content mitigates corrosion. The higher porosity contradiction led to further studies on the effect of porosity on corrosion resistance.

One aspect not considered in detail is the existence of interconnected porosity and its effect on the corrosion resistance. If a low-porosity coating were to exhibit a microstructure with interconnected porosity, it would have lower corrosion resistance than a higher porosity coating with homogeneous porosity. Several of the coatings were examined with both eddy-current techniques and acoustic microscopy in an attempt to quantify the amount of interconnected porosity in thermal spray coatings. Unfortunately, results are inconclusive at this time.

By substitution of Eq 1 and 2 into Eq 6, and Eq 4 into Eq 7, the complete parameter/property/performance relationship is established for both material systems, relating process parameters to the coating attributes and then to the actual coating performance.

7. Summary and Conclusions

A Box statistical experimental study of the twin-wire electric arc spraying of 85/15 and 70/30 zinc/aluminum wires has been presented. Major parameters investigated in the studies included gun orifice diameter, spray distance, current, and gun pressure. Coating attributes evaluated included porosity, roughness, oxide content, bond strength, and corrosion resistance. These studies led to optimized process parameters for the most corrosion resistant coatings.

The 85/15 and 70/30 material systems exhibited very similar coating properties and performance. The porosities of the 85/15 coatings ranged from 0.6 to 5.8%; the porosities of the 70/30 coatings ranged from 1.4 to 8.7%. The oxide content of the 85/15 coatings ranged from 0.3 to 3.9%. Average roughness was nominally 8 mm for the coatings. Deposition efficiency was 56.2% for the 85/15 coatings and 47% for the 70/30 coatings. The bond strength ranged from 5.61 to 10.11 MPa (814 to 1467 psi) for the systems. The 7030C coating has discernible porosity homogeneously dispersed throughout the coating matrix. Some large pores are evident. No cracking occurred. The 8515C coating has smaller pores than the 70/30 coating with a more homogeneous distribution. No cracking nor unmelted particles were evident.

Salt spray corrosion testing was conducted for 1000 h in accordance with ASTM B 117-95. The test panels were evaluated for surface pitting, percentage of surface area exhibiting pitting or other corrosive activity, erosion of coating from the edges,

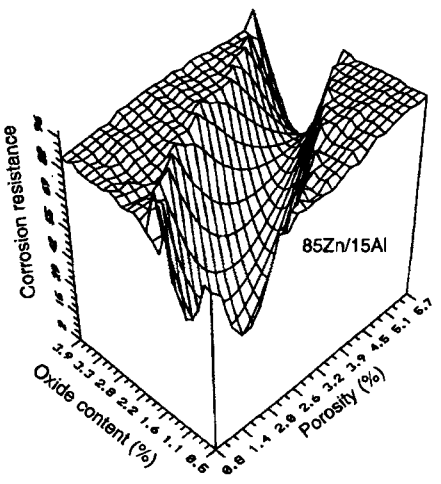

Fig. 5 85/15 corrosion resistance as a function of porosity and oxide content

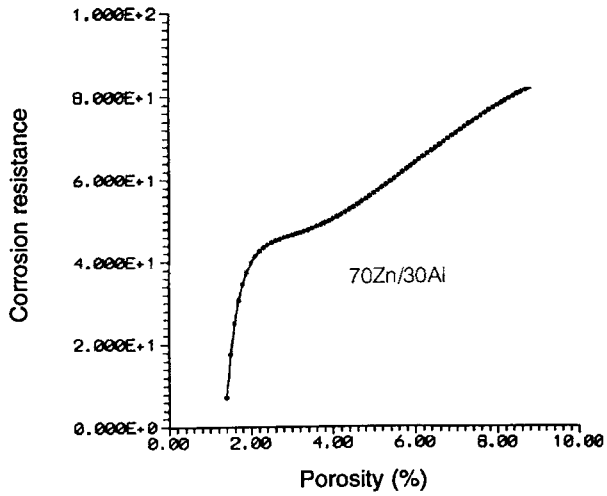

Fig. 6 70/30 corrosion resistance as a function of porosity

and whether the steel substrate was exposed. The 85/15 corrosion resistance was slightly higher than the 70/30 system.

The Box-type statistical design of experiment methodology was verified in confirmation testing. The optimum coating for this application would have high corrosion resistance. For the 70/30 system, corrosion resistance was most influenced by nozzle diameter. The combination of the blue nozzle cap, 0.55 MPa (80 psi) gun pressure, a current of 100 A, and a 17.8 cm (7 in.) spray distance produced the most corrosion resistant 70/30 coatings in the confirmation run with low porosity, intermediate roughness, and high bond strength. For the 85/15 system, corrosion resistance was affected primarily by nozzle diameter, with current and spray distance exhibiting a significant secondary effect. The combination of the green nozzle cap, 0.55 MPa (80 psi) gun pressure, a current of 100 A and a 7.62 cm (3 in.) spray distance produced the most corrosion resistant 85/15 coating in the confirmation run, with low porosity, low oxide content, low roughness, and intermediate bond strength.

Sequential regression analysis was used to establish a relationship between the process parameters, the coating microstructural attributes, and the coating corrosion performance. From the limited data of this study, correlation of the coating attributes with the performance evaluation was difficult and somewhat misleading. Corrosion resistance for 85/15 increased both as porosity and oxide content increased. The 70/30 alloy showed similar trends. However, based on the results from the effects analysis in this study and the subsequent confirmation testing, it is believed that the combination of lower porosity and oxide content mitigates corrosion. One aspect not considered in detail is the existence of interconnected porosity and its effect on the corrosion resistance.

The objective of this study was to demonstrate the use of thermal spray coatings for infrastructural applications. Baseline data were generated on factors that influence coating characteristics (i.e., porosity) and performance evaluation (i.e., corrosion resistance). Future work in this area will emphasize the regression analysis of coating attribute/performance relationship.

Acknowledgments

The assistance of D. Kunerth, C. Shelton-Davis, and L. Torres (INEEL) is gratefully acknowledged. The work described in this paper was supported by the U.S. Department of Energy, Assistant Secretary for Defense, under DOE Contract No. DE-AC07-94ID13223.

References

1. E.D. Kubel, *Adv. Mater. Process.*, Vol 132 (No. 6), December 1987, p 69-80
2. I. Suzuki, *Corrosion Resistant Coatings Technology,* Marcel Dekker, Inc., 1989
3. G.E.P. Box, W.G Hunter, and J.S. Hunter, *Statistics for Experimenters,* John Wiley & Sons, 1978
4. P. Whitcomb, et al., *Design-Ease,* version 2.0, Stat-Ease Inc., Minneapolis, MN 55413. Design-Ease is a registered trademark of Stat-Ease, Inc.
5. B.F. Ryan, B.L. Joiner, T.A. Ryan, Jr., Minitab Statistical Software, State College, PA, Duxburg Press, 1992.